Planta (2012) 235:995–1011
DOI 10.1007/s00425-011-1554-1

ORIGINAL ARTICLE

From callus to embryo: a proteomic view on the development and maturation of somatic embryos in *Cyclamen persicum*

Christina Rode · Kathrin Lindhorst · Hans-Peter Braun · Traud Winkelmann

Received: 25 July 2011 / Accepted: 4 November 2011 / Published online: 30 November 2011

Abstract In this study, the proteome structures following the pathway in somatic embryogenesis of *Cyclamen persicum* were analysed via high-resolution 2D-SDS-PAGE with two objectives: (1) to identify the significant physiological processes during somatic embryogenesis in *Cyclamen* and (2) to improve the maturation of somatic embryos. Therefore, the effects of maturation-promoting plant growth regulator abscisic acid (ABA) and high sucrose levels on torpedo-shaped embryos were investigated. In total, 108 proteins of differential abundance were identified using a combination of tandem mass spectrometry and a digital proteome reference map. In callus, enzymes related to energy supply were especially distinct, most likely due to energy demand caused by fast growth and cell division. The switch from callus to globular embryo as well as from globular to torpedo-shaped embryo was associated with controlled proteolysis via the ubiquitin-26S proteasome pathway. Storage compound accumulation was first detected 21 days after transfer to plant growth regulator (PGR)-free medium in early torpedo-shaped embryos. Increase in abundance of auxin-amidohydrolase during embryogenesis suggests a possible increase in auxin release in the late embryo stages of *Cyclamen*. A development-specific isoelectric point switch of catalases has been reported for the first time for somatic embryogenesis. Several proteins were identified to represent markers for the different developmental stages analysed. High sucrose levels and ABA treatment promoted the accumulation of storage compounds in torpedo-shaped embryos. Additionally, proteins of the primary metabolic pathways were decreased in the proteomes of ABA-treated embryos. Thus, ABA and high sucrose concentration in the culture medium improved maturation and consequently the quality of somatic embryos in *C. persicum*.

Keywords Abscisic acid · Development · Maturation · Somatic embryogenesis · Sucrose · Two-dimensional polyacrylamide gel electrophoresis

Abbreviations

2D	Two-dimensional
2iP	6-(γ-γ-Dimethylallylamino) purine
2,4-D	2,4-Dichlorophenoxyacetic acid
ABA	Abscisic acid
EDTA	Ethylenediaminetetraacetic acid
GAPDH	Glyceraldehyde-3-phosphate dehydrogenase
HSP	Heat shock protein
IEF	Isoelectric focusing
IPG	Immobilized pH gradients
LEA	Late embryogenesis abundant proteins
MS	Mass spectrometry
PGR	Plant growth regulator
RNase	Endoribonuclease
SDS-PAGE	Sodium dodecyl sulphate polyacrylamide gel electrophoresis
SERK	Somatic embryogenesis receptor like kinase

Electronic supplementary material The online version of this article (doi:10.1007/s00425-011-1554-1) contains supplementary material, which is available to authorized users.

C. Rode · H.-P. Braun
Institute of Plant Genetics, Leibniz Universität Hannover, Herrenhäuser Str. 2, 30419 Hannover, Germany

K. Lindhorst · T. Winkelmann (✉)
Institute of Floriculture and Woody Plant Science, Leibniz Universität Hannover, Herrenhäuser Str. 2, 30419 Hannover, Germany
e-mail: traud.winkelmann@zier.uni-hannover.de

SOD	Superoxide dismutase
TCA	Tricarboxylic acid
VDA channel	Voltage-dependent anion channel

Introduction

Cyclamen persicum is an economically important and popular ornamental crop. Unfortunately, the propagation of this plant via seeds is a labour- and cost-intensive process due to inbreeding depression of parents and genetically heterogeneous offsprings. Somatic embryogenesis is well characterised for *Cyclamen* and protocols for the in vitro production of embryos are established (Wicart et al. 1984; Kiviharju et al. 1992; Schwenkel and Winkelmann 1998; Prange et al. 2010a, b). Starting from embryogenic callus, the removal of auxin, i.e. the culture on plant growth regulator (PGR) free medium, leads to the realisation of embryogenesis undergoing the typical stages as globular and finally torpedo-shaped embryos within 4 weeks (Schmidt et al. 2006). After germination of these embryos healthy and genetically identical plants can be transferred to the greenhouse. A large-scale propagation of *Cyclamen* via this technique is an obvious aim. However, physiological disorders in a relevant portion of emerged embryos as well as asynchronous development limit the commercial application so far. To better control these factors profound knowledge of the physiology of embryogenesis is essential.

Proteomic studies have been shown to be powerful tools for monitoring the physiological status of plant organs under specific developmental conditions (Rose et al. 2004). A proteomic dissection of somatic embryogenesis has been performed for some major crops in the last years (*Quercus*, Mauri and Manzanera 2003; *Medicago*, Imin et al. 2005; *Picea*, Lippert et al. 2005; soybean, Hajduch et al. 2005; *Vitis*, Marsoni et al. 2008; date palm, Sghaier-Hammami et al. 2010). For *Cyclamen*, initial (Winkelmann et al. 2006) and large-scale analyses (Rode et al. 2011) comparing the proteomes of somatic and zygotic embryos as well as embryogenic and non-embryogenic callus (Lyngved et al. 2008) have been performed previously. Data published on these studies provided important insights into *Cyclamen* embryogenesis. However, a proteomic view on the different stages of this developmental process, from callus to embryo, is still missing.

Somatic embryos of *C. persicum* have been shown to lack maturation-related characteristics like the accumulation of storage compounds (Winkelmann et al. 2006; Rode et al. 2011), desiccation (Winkelmann et al. 2004) and a quiescence period (Schmidt et al. 2006). This may correlate with inhomogeneous development and premature germination. Some promising studies demonstrated maturation-promoting effects of high sucrose concentration in the culture media during embryo development (Klimaszewska et al. 2004; Winkelmann et al. 2006; Sghaier-Hammami et al. 2010) as well as of abscisic acid (ABA) treatment after embryo differentiation (Gutmann et al. 1996; Garcia-Martin et al. 2005; Vahdati et al. 2008; Sghaier-Hammami et al. 2010).

The aim of this study was to elucidate the physiological key processes during the somatic embryogenesis of *Cyclamen*. Additionally, the effects of ABA and sucrose treatments on somatic embryos were investigated. The proteomes of different developmental stages of somatic embryos were analysed via a gel-based proteomic approach and proteins were identified using a combination of tandem mass spectrometry and the digital reference map for *C. persicum* embryos (Rode et al. 2011; http://www.gelmap.de/cyclamen).

Materials and methods

Plant material and experimental setup

Embryogenic callus and subsequent developing somatic embryos were derived from the *C. persicum* commercial F_1 cultivar 'Maxora Light Purple' bred by the company Varinova B.V. (Berkel en Rodenrijs, Netherlands). Embryos were produced from embryogenic suspension cultures grown in half-strength liquid Murashige and Skoog (1962) medium, containing FeEDTA at full strength, pH 5.5–5.6, 30 g l^{-1} sucrose, 2 g l^{-1} glucose, 2.0 mg l^{-1} 2,4-D and 0.8 mg l^{-1} 2iP as described by Winkelmann et al. (1998).

For induction of embryogenesis, 1 ml of a 500–1,000 µm cell fraction of the suspension washed in liquid plant growth regulator (PGR) free medium of the same basal composition and adjusted to a density of 10% packed cell volume was plated onto PGR-free medium (30 ml in 9 cm Petri dishes) solidified with 4 g l^{-1} Gelrite (Duchefa, Haarlem, Netherlands). Sucrose was added to this medium in two different concentrations: 30 and 60 g l^{-1}. Medium and cells were separated by a disc of 100 µm nylon mesh (Neolab, Heidelberg, Germany).

For the time course experiment (Exp. A, Fig. 1) embryogenic cells were incubated at 24°C in the dark on both solid media containing 30 and 60 g l^{-1} sucrose. The cells and developing somatic embryos were harvested after 0, 1, 3, 7, 21 and 28 days of incubation.

For the abscisic acid (ABA; (+)-*cis*,*trans* ABA, A0941, Duchefa) experiment (Exp. B, Fig. 1) 28-day-old embryos that had developed on medium containing 30 g l^{-1} sucrose were transferred to a medium of the same composition, with or without 10 mg l^{-1} ABA. On these media, the embryos were incubated for further 28 days at 24°C in the dark. Thus, they were 56 days old at harvesting time.

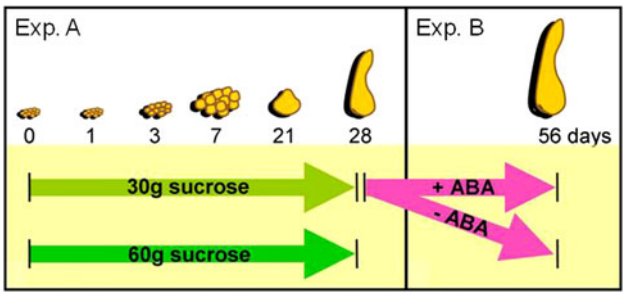

Fig. 1 Experimental setup. *Exp. A* Time course experiment: somatic embryos were induced from embryogenic suspension cells plated on solid PGR-free medium containing 30 or 60 g l^{-1} sucrose. Tissue for proteomic analysis was harvested for 6 developmental stages (0, 1, 3, 7, 21 and 28 days after transfer to PGR-free medium) from both sucrose variants. *Exp. B* ABA treatment: 28-day-old embryos grown on medium containing 30 g l^{-1} sucrose were transferred to medium additionally containing 0 or 10 mg l^{-1} abscisic acid (*ABA*). These embryos were harvested after 4 weeks with these additional treatments for proteomic analysis

From each of the developing stages 100 mg of material was harvested and directly frozen in liquid nitrogen. Therefore, complete cell clusters were collected for the developing stages 0, 1, 3 and 7 days. For the developing stages 21, 28 and 56 days torpedo-shaped embryos were selected by hand under a stereomicroscope (Zeiss, Jena, Germany).

Each experiment (A and B) was repeated three times using biologically independent tissue. Thus, three biological replicates for each of the developing stages and media were used for protein extraction resulting in $3 \times 13 = 39$ 2D-SDS-PAGEs in total.

Phenolic protein extraction and sample preparation for IEF

Total protein extraction and sample preparation for IEF was performed as described by Rode et al. (2011). Proteins were extracted from 100 mg fresh tissue according to the protocol of Hurkman and Tanaka (1986) modified by Colditz et al. (2005) using phenol combined with ammonium acetate in methanol precipitation.

2D IEF/SDS-PAGE and protein staining

For the first dimension, isoelectric focusing, complete protein fractions extracted from 100 mg of fresh tissue were loaded on Immobiline^{TM} DryStrip gels [18 cm, pH gradient (pH 3–11, non-linear) (GE Healthcare, Freiburg, Germany)] and isoelectrically focussed for 24 h with voltages from 30 to 8,000 V at maximum according to Mihr and Braun (2003) using the IPGphor system (GE Healthcare). For the second dimension separation (SDS-PAGE), IPG strips were equilibrated and placed horizontally on a 12% tricine SDS-PAGE gel. Electrophoresis was carried out for 20 h at 30 mA mm^{-1} gel layer using the Biorad Protean II XL gel system (Biorad, Muenchen, Germany). Subsequently proteins were stained with colloidal Coomassie Blue 250 G (Merck, Darmstadt, Germany) (Neuhoff et al. 1985, 1990). For further details see Rode et al. (2011).

2D gel analyses

Gels were scanned and analysed using Delta 2D version 4.2 software (Decodon, Greifswald, Germany). For the 33 gels resulting from the time course experiment (experiment A), spot detection was achieved automatically on a digitally fused image of all 33 gels. Finding an adequate and common spot detection for all developmental stages of the time course experiment (experiment A), required a strict spot filter application. Thus, only the spots with the highest volume and quality (spots with a relative volume less than 0.015% and a spot quality less than 0.4 were discarded) were transferred from the overlay image to all gels of the time course experiment. Spot detection for the gels resulting from the ABA experiment (experiment B) was achieved separately, since especially the proteomes of the early development stages and the 56-day-old embryos were hardly comparable. Due to the fact that the six gels from experiment B represented less heterogeneous tissues as compared to those analysed in experiment A, a less strict spot filter was applied. Here, spots with a relative volume less than 0.005% were discarded. After manual correction spot detection was transferred from the fused image (of all six gels of the ABA experiment) to all single gels of the ABA experiment.

In both experiments (A and B) all gels of one developmental stage were combined to one group. Groups were compared pair wise. For determination of significant alterations in the spot patterns between two groups, a Student's *t* test was performed (confidence interval $\geq$ 95%) based on the relative spot volume. From the protein spots which had a statistically significant different abundance, only those with at least 1.5-fold alterations in protein abundance were considered to represent true differences and further considered.

Protein identification

Differentially abundant proteins were identified via tandem mass spectrometry for the early embryo stages (days 1, 2 and 7) using a nano high-performance liquid chromatography (Proxeon, Thermo Scientific, Dreieich, Germany) electrospray ionization quadrupole time of flight system (micrOTOF Q II MS, Bruker Daltonics, Bremen, Germany). Subsequent database search was carried out via the Mascot search engine in the NCBInr-plants (http://www.ncbi.nlm.nih.gov/) and the TAIR10 databases (http://www.arabidopsis.org). A detailed description for in-gel

protein digestion, mass spectrometry and database search is given in Supplement S1. For the torpedo-shaped embryos (days 21, 28, 56) protein identification was performed using the proteome reference map for torpedo-shaped embryos of *C. persicum* (Rode et al. 2011; http://www.gelmap.de/cyclamen). Therefore, the IEF SDS-PAGE of the reference map was matched to the gels analysed in our study using Delta 2D software. Hereupon, the spot labels containing the proteins' names were transferred from the reference map to the corresponding spots of the gels analysed here.

Results

The first aim of this study was to analyse the developmental changes during somatic embryogenesis in *C. persicum* from a physiological point of view.

Development of somatic embryos

One and 3 days after transferring the cells to PGR-free MS medium, they appeared arrested in growth and showed no morphological changes (Fig. 2a, first row, 1d and 3d). But already after 7 days on PGR-free MS medium small globular embryos were visible (Fig. 2a, first row, 7d). These embryos were enlarged after 21 days on PGR-free MS medium and some had a drop-like shape due to the developing cotyledon (Fig. 2a, first row, 21 d). After 28 days the cotyledon had elongated and the embryos displayed the torpedo shape. There were no significant morphological differences between cells/embryos grown on 30 and 60 g l^{-1} sucrose during the first 3 weeks. However, after 28 days the embryos grown on 60 g l^{-1} sucrose were smaller, seemed to be denser and less swollen compared to their counterparts grown on 30 g l^{-1} sucrose.

When ABA-treated embryos were compared to non-treated ones, no significant morphological alteration could be detected except that the root pole and first developing roots started to turn brownish on ABA containing medium. The 56-day-old embryos were slightly larger compared to their 28-day-old pendants. The germination of the embryos did not take place in our experiments because the embryos were not separated.

Quantitative analysis of 2D-PAGEs and protein identification

Separation by IEF SDS-PAGE led to a resolution of more than 1,000 protein spots per gel. Overlays of three replicates of the 2D-PAGEs for each developmental stage of the time course experiment (experiment A) are shown in Fig. 2a (second row) in comparison to callus (day 0).

Fig. 2 **a** Alterations in protein abundances during somatic embryogenesis. *First row* developing embryos cultivated on 60 g l^{-1} sucrose are shown 1–28 days after transfer to PGR-free MS medium. Each picture was taken at ×20 magnification. *Bars* 1 mm. *Second row* overlays of IEF SDS-PAGEs of embryogenic callus cultivated on PGR-containing medium (=day 0) and the five developmental stages are shown in pair-wise comparisons. Spots with similar abundance in both tissues appear in *yellow*, those with higher abundance in the embryogenic callus cultivated on PGR-containing medium in *purple* and spots with a higher abundance in tissue of the respective stage appear in *green*. *Third row* only those spots are labelled which were at least 1.5-fold significantly higher abundant in one of the two compared tissues. *Green-labelled* spots were at least 1.5-fold more abundant in the developing tissue/embryo proteomes and *purple-labelled* spots were at least 1.5-fold more abundant in the callus proteome. The *numbers at the bottom* indicate the number of significantly higher abundant spots in the compared tissues. Spots of major interest discussed in detail in the text are indicated. **b** Alterations in protein abundances of 28-day-old torpedo-shaped embryos and embryogenic callus. Enlarged picture of the overlay for 28-day-old torpedo-shaped embryos and embryonic callus shown in **a** in the *third row*, last picture *right*. *Green-labelled* are embryo proteins, *purple-labelled* callus proteins

Herein, only the results for the tissues grown on 60 g l^{-1} sucrose are shown, since only few significant differences could be detected from tissues grown on 30 g l^{-1}, except for the 28-day-old somatic embryos. Therefore, 28-day-old embryos of the 60 g l^{-1} sucrose treatment were contrasted with embryos of the same age grown on medium containing 30 g l^{-1} sucrose (Fig. 3).

In total 331 spots were included in the statistical evaluation of the time course experiment (experiment A). Since important physiological events were expected especially for the first stages (days 1, 3, and 7), all 39 proteins of these three stages showing significant differences in abundance compared to callus (day 0) were analysed by tandem mass spectrometry. The numbers of differentially abundant proteins for the various tissue comparisons are given in Table 1. Overall, 47% of the proteins differing in abundance could be identified using tandem mass spectrometry and the proteome reference map published by Rode et al. (2011) (Table 1).

Within the 39 spots analysed via mass spectrometry proteins were identified in 32 of them representing 82% identification rate (Supplementary Table S2). Hereof four proteins had already been identified via the proteome reference map resulting in the same protein species (ID365/35; ID17829/39, ID750/18 and ID387/6), four proteins were additionally identified in the same spot, and in 24 spots proteins were identified for the first time; however, four of them represented "uncharacterised" protein species.

In total, 667 spots were included in the evaluation of experiment B whereof 43 spots were differentially abundant and 15 could be identified using the proteome reference map published by Rode et al. (2011) (Table 1, Exp. B).

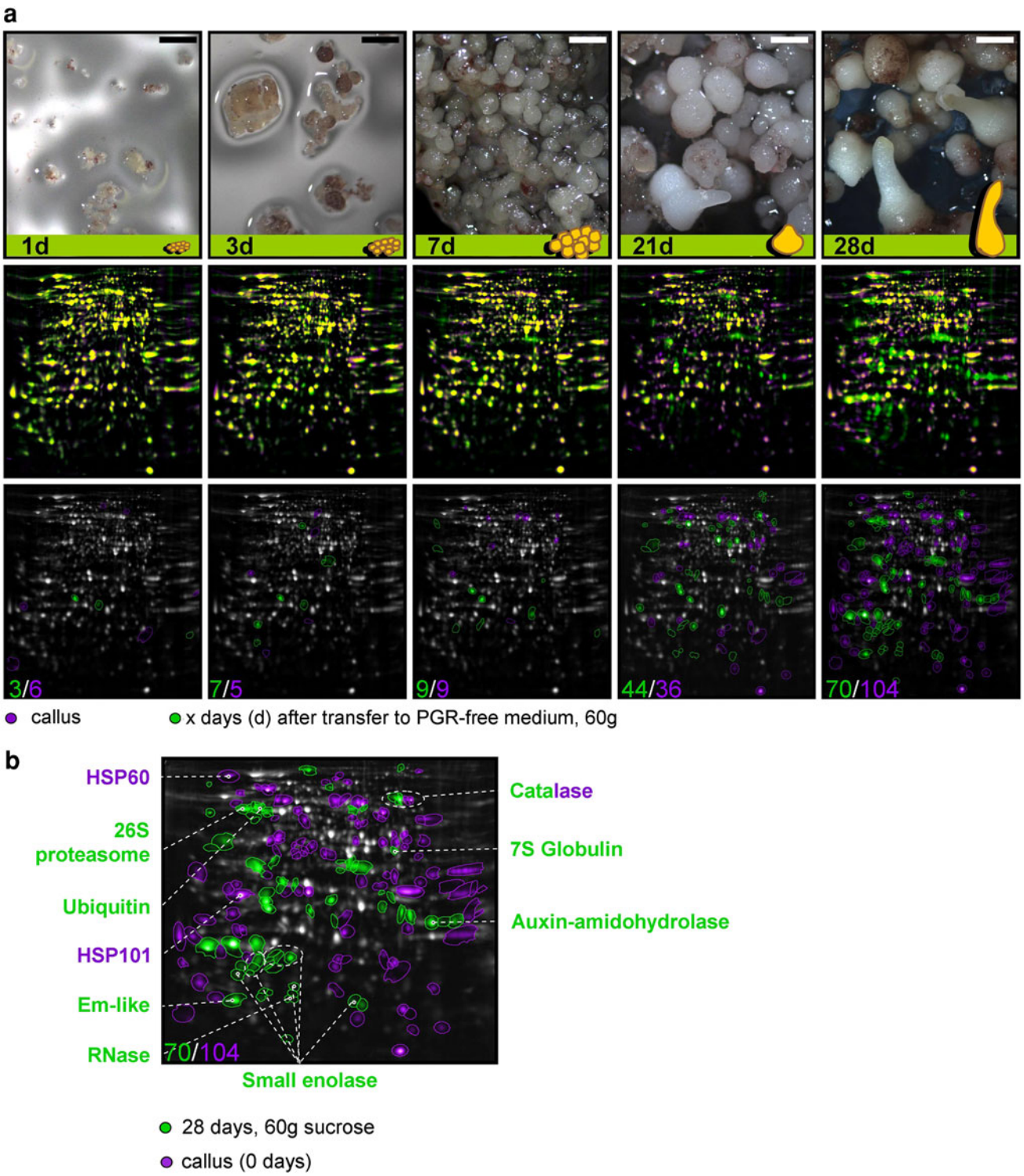

Proteomic changes during the development of somatic embryos (experiment A)

One day after transfer to PGR-free MS medium, nine protein spots differed significantly in their abundance. For the progressing developmental stages, their number increased steadily (Table 1, Exp. A; Fig. 2, 3rd row). The rise of differentially abundant spots was especially pronounced in the late development stages: 21 days (80 spots) and 28 days (173 spots). All identified proteins that expressed significant changes in abundance as well as their relative spot volumes are given in Table 2.

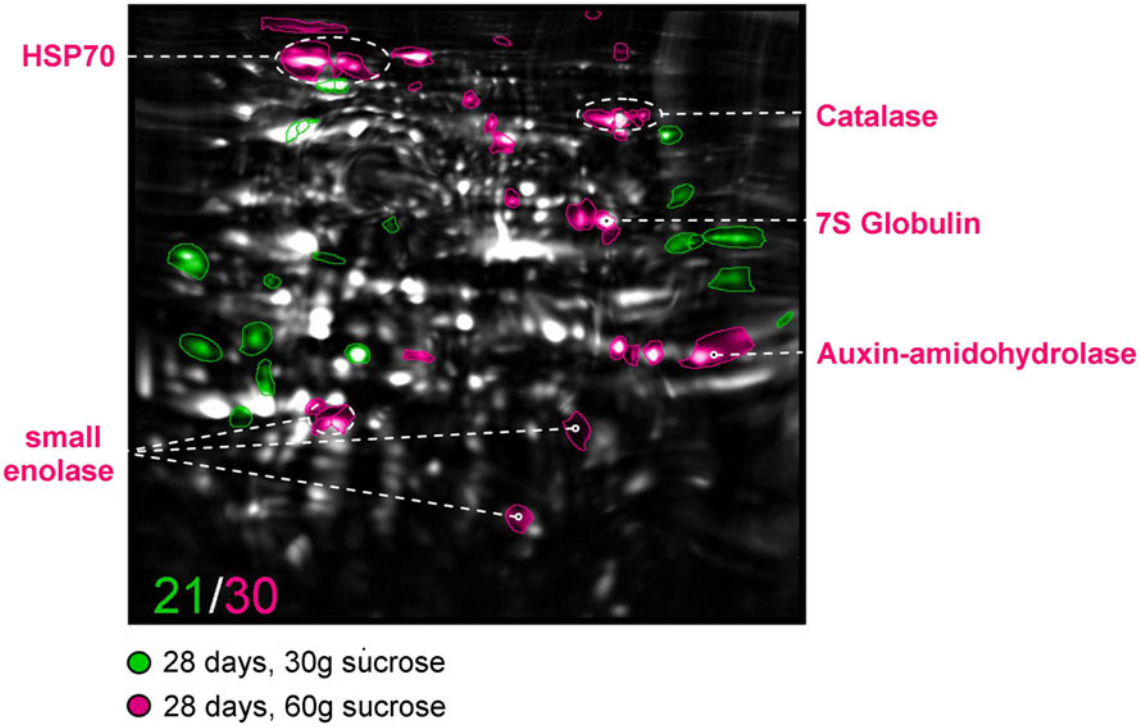

Fig. 3 Alterations in protein abundances in 28-day-old embryos cultivated on MS medium containing 30 or 60 g l^{-1} sucrose (three replicates, each). Overlay image of IEF SDS-PAGE of callus and 28-day-old embryo proteomes using Delta2D software. *Green-labelled* spots were at least 1.5-fold more abundant in the proteome of embryos cultivated with the lower sucrose concentration (30 g l^{-1}) and *pink-labelled* spots were at least 1.5-fold more abundant in the proteome of embryos cultivated with higher sucrose concentration (60 g l^{-1}). Spots of major interest discussed in detail in the text are indicated

Table 1 Total numbers of identified proteins

Experiment	Tissues to be compared	Differentially abundant proteins[a]	Proteins identified via reference map[b]	Proteins identify via MS[c]	Total number of identified proteins[d]
A 1	Callus vs.				
	1 day (60 g)	9	4	5	6
	3 days (60 g)	12	2	10	10
	7 days (60 g)	18	6	17	20
	21 days (60 g)	80	33	Not performed	33
	28 days (60 g)	173	70	Not performed	70
A 2	28 days (30 g) vs.				
	28 days (60 g)	51	26	Not performed	26
B	56 days (30 g) vs.				
	56 days (30 g + ABA)	43	15	Not performed	15

[a] Number of differentially abundant proteins. For experiment A1 and A2 in total 331 spots were included in the evaluation. For experiment B in total 667 spots were included in the evaluation

[b] Differentially abundant proteins were identified using the *Cyclamen persicum* embryo proteome reference map (Rode et al. 2011; http://www.gelmap.de/cyclamen) for all developmental stages

[c] Differentially abundant proteins were identified via mass spectrometry for days 1, 3 and 7 (Supplement S1, Suppl. Table S1, Suppl. Fig. S1)

[d] Total number of proteins identified using mass spectrometry and the digital reference map. In case one protein was identified with both approaches it is considered only once

Table 2 Protein abundances during the development of somatic embryos from callus to torpedo-shaped embryo

			0 days		1 day			3 days			7 days			21 days			28 days			
protein name[a]	MW[b]	ID[c]	v[d]	cov[e]	v[d]	cov[e]	ratio[f]	v[d]	cov[e]	ratio[f]	v[d]	cov[e]	ratio[f]	v[d]	cov[e]	ratio[f]	v[d]	cov[e]	ratio[f]	
26S protease regulatory subunit 6B homolog	m	ID20	0.2	37	0.3	33	1.8	0.4	25	2.3	0.3	31	2.0	0.3	14	1.7	0.2	33	1.0	
26S protease, subunit 6B	m	ID1957	0.3	6	0.3	13	1.0	0.4	5	1.3	0.4	12	1.4	0.3	14	1.1	0.5	20	1.6	
26S proteasome, subunit 7	m	ID1970	0.1	5	0.1	25	0.9	0.1	9	1.1	0.2	50	1.8	0.2	30	2.3	0.3	25	2.8	
7S globulin	s	ID8764	0.0	21	0.0	22	.	0.0	44	.	0.0	56	.	0.3	21	.	0.6	35	.	
Actin 1	l	ID456	0.1	9	0.2	85	2.1	0.1	10	0.8	0.1	21	1.0	0.2	33	1.5	0.3	20	2.5	
Alcohol dehydrogenase	m	ID558	0.2	18	0.2	17	0.8	0.2	1	0.9	0.2	14	0.8	0.2	32	0.8	0.1	24	0.6	
Aldehyde dehydrogenase	m	ID38	0.9	13	0.8	20	0.9	0.8	6	0.8	0.6	20	0.6	0.5	26	0.6	0.6	13	0.6	
Aldehyde dehydrogenase	m	ID387; ID6	0.1	32	0.0	16	0.3	0.1	20	0.6	0.1	29	0.7	0.1	24	0.8	0.1	12	0.9	
Anthocyanidin reductase	m	ID32	0.2	13	0.2	4	1.2	0.2	8	0.8	0.1	10	0.7	0.1	21	0.7	0.1	24	0.5	
Anti-Oxidant 1	m	ID1074	0.7	18	0.4	42	0.6	0.4	21	0.7	0.7	43	1.0	0.9	31	1.3	1.0	14	1.5	
ATPase subunit 1; Pyruvate kinase	m, m	ID21; ID37	0.4	16	0.3	4	0.7	0.3	17	0.6	0.2	16	0.6	0.3	10	0.7	0.2	22	0.6	
Auxin-amidohydrolase	s	ID853	0.1	38	0.1	42	0.9	0.2	11	1.1	0.3	66	1.9	0.6	43	3.8	1.5	18	10.4	
Beta-ketoacyl-ACP synthase I	m	ID516	0.1	26	0.1	22	1.0	0.1	22	1.1	0.1	4	1.4	0.1	27	1.9	0.1	25	1.3	
Calmodulin	m	ID938	1.3	11	1.1	53	0.8	0.8	52	0.6	1.1	46	0.8	1.0	41	0.7	0.7	17	0.6	
Catalase	m	ID17829; ID39	0.2	17	0.2	14	0.8	0.1	26	0.7	0.1	5	0.6	0.1	37	0.5	0.1	11	0.5	
Catalase	m	ID386	0.3	27	0.3	14	1.2	0.4	1	1.3	0.5	32	1.6	0.6	10	2.1	0.6	16	2.2	
Catalase	m	ID389	0.3	7	0.3	25	1.0	0.3	31	0.8	0.2	7	0.6	0.2	45	0.7	0.2	14	0.5	
Catalase	m	ID392	0.1	56	0.2	14	1.6	0.1	14	1.2	0.2	47	1.8	0.3	18	2.6	0.4	16	4.1	
Cell division control protein	m	ID499	0.1	35	0.1	38	1.5	0.1	38	1.9	0.1	40	2.0	0.1	8	2.1	0.1	23	1.2	
Co-chaperone GrpE family protein	m	ID31	0.0	114	0.0	99	0.7	0.0	66	1.0	0.1	47	8.3	0.1	21	3.8	0.1	48	9.7	
Copper/zinc SOD	s	ID1003	0.3	12	0.3	13	1.0	0.4	8	1.2	0.3	53	1.0	0.2	44	0.6	0.1	22	0.3	
eIF(iso)4E*	m	ID830	0.3	23	0.2	10	0.9	0.3	10	1.1	0.3	26	1.2	0.5	29	1.7	0.9	14	3.5	
Elongation factor 1-alpha	s	ID959	1.1	23	1.0	17	0.9	1.2	20	1.1	1.5	17	1.3	1.3	23	1.2	2.2	14	2.0	
Em-like protein	s	ID1059	0.0	50	0.0	29	1.4	0.0	47	0.9	0.0	40	1.9	0.0	61	1.7	0.1	53	4.3	
Enolase	s	ID1020	0.0	93	0.0	100	0.6	0.0	66	2.2	0.1	58	4.7	0.2	24	7.8	0.3	16	15.4	
Enolase	s	ID1022	0.1	36	0.0	85	0.7	0.1	14	1.0	0.1	35	1.4	0.1	28	1.4	0.2	9	3.5	
Enolase	l	ID1043	0.0	39	0.0	16	0.6	0.0	23	0.4	0.0	16	0.5	0.0	45	0.8	0.1	10	2.4	
Enolase	s	ID1083	0.0	76	0.0	52	2.0	0.0	41	1.4	0.0	84	3.9	0.1	50	10.5	0.3	19	24.3	
Enolase	m	ID11657	0.2	9	0.3	38	1.2	0.2	10	1.1	0.3	23	1.3	0.3	37	1.5	0.4	17	2.1	
Enolase	s	ID18597	0.8	27	0.8	24	1.0	0.8	9	1.0	1.0	29	1.2	1.3	33	1.6	1.9	15	2.3	
Enolase	l	ID353	0.1	23	0.0	12	0.6	0.1	1	0.8	0.1	45	1.2	0.1	45	1.7	0.2	5	2.2	
Enolase	m	ID480	0.9	6	1.0	17	1.1	1.0	14	1.1	1.0	15	1.1	1.4	18	1.6	1.1	24	1.2	
Enolase	s	ID641	0.4	18	0.4	18	1.1	0.4	16	1.0	0.4	20	0.9	0.4	20	0.9	0.2	10	0.6	
Enolase	s	ID803	0.1	16	0.1	21	0.9	0.1	14	1.0	0.1	25	0.9	0.1	31	1.2	0.3	27	3.6	
Enolase	s	ID8980	0.0	27	0.0	31	0.7	0.0	32	0.7	0.1	89	2.1	0.1	42	4.3	0.2	32	8.8	

Table 2 continued

			0 days		1 day			3 days			7 days			21 days			28 days			
protein name[a]	MW[b]	ID[c]	v[d]	cov[e]	v[d]	cov[e]	ratio[f]	v[d]	cov[e]	ratio[f]	v[d]	cov[e]	ratio[f]	v[d]	cov[e]	ratio[f]	v[d]	cov[e]	ratio[f]	
Enolase	s	ID8980	0.0	27	0.0	31	0.7	0.0	32	0.7	0.1	89	2.1	0.1	42	4.3	0.2	32	8.8	
Enolase	s	ID976	0.2	19	0.2	11	0.9	0.2	15	0.8	0.1	36	0.6	0.1	26	0.5	0.1	36	0.4	
Enolase	s	ID981	0.1	25	0.1	19	1.1	0.1	13	1.3	0.1	5	1.6	0.2	34	1.9	0.4	13	4.5	
Enolase	s	ID983	0.3	8	0.4	9	1.2	0.3	23	1.0	0.3	27	0.8	0.2	43	0.6	0.1	62	0.4	
Enolase	s	ID986	0.4	43	0.6	11	1.7	0.7	28	1.9	0.8	24	2.0	0.8	8	2.2	0.7	22	1.8	
Enolase	s	ID997	0.1	16	0.1	13	0.9	0.1	44	1.0	0.1	42	1.9	0.2	59	2.7	0.6	15	7.8	
Enolase; HSP 20 (groes chaperonin)	s, m	ID863; 28	0.4	20	0.5	3	1.2	0.5	9	1.3	0.8	28	1.9	1.2	38	2.9	1.2	36	2.9	
Fructose-bisphosphate aldolase	m	ID566	0.4	7	0.6	6	1.3	0.5	12	1.2	0.6	32	1.4	0.8	11	1.9	0.6	17	1.4	
Fructose-bisphosphate aldolase	m	ID568	0.9	15	1.2	12	1.3	1.1	8	1.2	1.1	10	1.2	1.4	9	1.6	1.0	16	1.1	
GAPDH	s	ID16803	0.3	16	0.3	25	1.1	0.3	6	1.1	0.3	16	1.0	0.3	44	1.0	0.7	27	2.4	
GAPDH	l	ID199	0.1	59	0.0	77	0.5	0.2	66	1.7	0.3	76	2.9	0.6	68	5.9	0.9	14	8.0	
GAPDH	m	ID600	0.3	18	0.4	10	1.3	0.4	18	1.2	0.4	8	1.2	0.5	4	1.6	0.5	14	1.5	
GAPDH	m	ID602	0.5	26	0.4	4	0.8	0.3	25	0.7	0.3	25	0.6	0.3	17	0.6	0.2	36	0.5	
GAPDH	m	ID607	0.5	27	0.5	16	1.1	0.4	17	0.9	0.4	21	0.7	0.4	37	0.8	0.3	45	0.5	
GAPDH	m	ID615	0.5	10	0.5	2	1.0	0.5	9	0.9	0.4	17	0.8	0.3	5	0.6	0.2	18	0.4	
GAPDH	m	ID626	0.4	20	0.3	13	0.8	0.3	8	0.8	0.2	16	0.6	0.2	31	0.5	0.1	18	0.3	
GAPDH	s	ID714	0.1	29	0.1	25	0.8	0.1	27	0.8	0.1	22	0.8	0.1	15	0.8	0.0	34	0.5	
GAPDH	s	ID757	0.1	20	0.1	64	0.9	0.1	28	0.9	0.2	101	2.8	0.4	57	5.9	1.4	34	21.8	
GAPDH	m	ID8929	0.5	8	0.5	12	1.1	0.5	14	0.9	0.4	18	0.8	0.3	8	0.6	0.3	9	0.5	
Glutathione reductase	m	ID414	0.7	12	0.6	7	0.8	0.6	5	0.8	0.5	6	0.7	0.5	13	0.6	0.4	18	0.6	
Histone H4; Protein translation factor SUI1	m, m	ID8; ID26	0.0	53	0.1	22	3.7	0.0	63	3.0	0.1	41	3.7	0.1	55	3.9	0.0	167	1.5	
Histone superfamily protein	l	ID19	0.1	3	0.1	63	0.7	0.0	39	0.3	0.1	6	1.0	0.1	54	1.1	0.1	38	0.8	
HSP 101	s	ID787	1.7	29	2.0	33	1.2	2.1	24	1.3	1.4	28	0.9	1.0	21	0.6	1.0	14	0.6	
HSP 20	m	ID879	0.2	18	0.3	44	1.1	0.2	44	0.8	0.2	23	1.0	0.4	26	1.7	1.0	19	3.9	
HSP 20	l	ID880	0.6	25	0.6	7	0.9	0.7	8	1.1	0.7	32	1.0	0.5	35	0.8	0.2	18	0.3	
HSP 20	m	ID947	0.9	11	1.3	29	1.4	1.2	9	1.3	1.3	20	1.5	1.4	15	1.6	1.3	14	1.4	
HSP 20	m	ID985	0.0	56	0.0	118	0.7	0.1	60	1.8	0.1	14	2.2	0.1	26	2.0	0.2	16	7.0	
HSP 20; Peroxiredoxin, Type IIF; Eukaryotic initiation factor 4A-9	m, m, s	ID897; ID4; ID15	0.4	27	0.7	18	2.0	0.9	30	2.5	0.9	25	2.6	0.8	6	2.3	0.5	28	1.3	
HSP 60	m	ID355	0.6	9	0.6	21	1.0	0.5	11	0.9	0.4	17	0.7	0.4	13	0.6	0.3	20	0.5	
HSP 60	m	ID365; 35	0.2	5	0.2	17	0.9	0.2	9	0.9	0.2	6	0.9	0.2	17	0.9	0.2	20	0.7	
HSP 70	s	ID7469	0.3	8	0.4	21	1.0	0.4	14	1.0	0.5	47	1.4	0.6	46	1.8	1.1	23	3.1	
Malate dehydrogenase	s	ID1310	0.1	17	0.1	21	1.1	0.2	14	1.2	0.5	90	3.7	0.4	74	2.7	1.0	48	7.1	
Malate dehydrogenase	m	ID648	0.2	15	0.2	8	1.1	0.2	7	1.1	0.2	21	1.0	0.2	53	1.0	0.1	38	0.4	
Manganese SOD	s	ID858	0.2	37	0.2	7	1.1	0.2	25	1.1	0.3	53	1.7	0.6	16	3.0	1.0	14	5.1	
Monodehydroascorbate reductase	s	ID473	0.6	19	0.5	6	0.9	0.5	20	0.9	0.5	19	0.9	0.5	24	0.8	0.3	15	0.6	

Table 2 continued

			0 days		1 day			3 days			7 days			21 days			28 days			
protein name[a]	MW[b]	ID[c]	v[d]	cov[e]	v[d]	cov[e]	ratio[f]	v[d]	cov[e]	ratio[f]	v[d]	cov[e]	ratio[f]	v[d]	cov[e]	ratio[f]	v[d]	cov[e]	ratio[f]	
Nucleoside diphosphate kinase	s	ID1001	0.1	19	0.1	4	0.9	0.1	27	0.7	0.1	20	0.7	0.1	16	0.7	0.1	30	**0.6**	
Nucleoside diphosphate kinase	m	ID24	0.0	35	0.0	64	0.7	0.0	67	**0.3**	0.0	70	**0.1**	0.0	93	1.4	0.0	56	1.5	
Nucleoside diphosphate kinase[a]; Ubiquitin-40S [b]	s, m	ID1024; 7	0.4	19	0.2	15	**0.6**	0.3	22	0.8	0.3	16	0.8	0.2	32	**0.6**	0.2	20	**0.5**	
Peptidyl-prolyl cis-trans isomerase	m	ID9	0.2	18	0.1	6	**0.5**	0.1	25	0.8	0.1	35	0.8	0.1	16	0.9	0.1	44	**0.4**	
Peptidyl-prolyl cis-trans isomerase	s	ID941	1.7	20	1.7	12	1.0	1.8	5	1.0	2.1	13	1.2	1.9	17	1.1	1.0	15	**0.6**	
Phosphoglycerate kinase	s	ID9067	0.0	13	0.0	79	0.4	0.0	53	0.6	0.0	37	1.1	0.0	55	2.4	0.2	18	**8.6**	
Phosphoserine aminotransferase	m	ID33	0.4	10	0.4	25	1.0	0.3	20	0.8	0.3	6	**0.6**	0.2	33	**0.5**	0.1	23	**0.4**	
Polygalacturonase	l	ID3278	0.3	29	0.4	31	1.2	0.4	40	1.2	0.7	31	2.0	0.6	25	**1.8**	0.8	11	**2.4**	
Prefoldin subunit 2	m	ID23	0.1	25	0.1	19	1.1	0.1	13	1.3	0.1	5	**1.6**	0.2	34	1.9	0.4	13	**4.5**	
Proteasome	m	ID412	0.2	26	0.2	18	1.0	0.2	13	1.2	0.3	57	1.9	0.5	33	**3.1**	0.6	13	**3.8**	
Proteasome	s	ID804	0.3	9	0.4	13	1.2	0.4	16	1.3	0.7	38	2.0	1.2	43	**3.5**	1.7	22	**5.1**	
RNase	s	ID1057	0.0	75	0.0	32	0.7	0.0	83	0.6	0.0	87	0.6	0.0	77	2.5	0.1	26	**9.5**	
Stress-inducible protein	m	ID299	0.2	22	0.2	30	1.2	0.3	13	1.3	0.3	22	1.3	0.2	20	1.0	0.1	38	**0.6**	
Succinate dehydrogenase	m	ID317	0.1	29	0.1	17	1.0	0.1	9	1.0	0.1	23	0.7	0.1	39	0.5	0.1	22	**0.5**	
Superoxide dismutase, (Cu-Zn)	m	ID12	0.3	25	0.4	39	1.1	0.6	1	**1.7**	0.4	46	1.3	0.3	42	0.7	0.2	23	**0.6**	
Triosephosphate isomerase	s	ID771	0.1	27	0.1	16	1.4	0.1	15	1.4	0.2	33	1.6	0.3	38	**2.6**	0.7	29	**7.0**	
Triosphosphate isomerase, type II	m	ID30	0.0	23	0.0	49	1.1	0.0	14	1.2	0.1	20	**1.9**	0.1	41	**3.2**	0.1	46	**3.9**	
Ubiquitin	s	ID1194	1.3	17	1.3	18	1.0	1.1	5	0.9	1.1	24	0.9	0.8	17	**0.6**	0.6	35	**0.4**	
Ubiquitin	l	ID810	0.1	50	0.1	15	1.0	0.0	81	0.4	0.0	55	0.5	0.1	40	**1.3**	0.4	26	**4.5**	
Ubiquitin	l	ID9986	0.4	20	0.4	29	1.0	0.4	1	1.0	0.4	34	1.2	0.6	32	1.6	0.8	20	**2.2**	
Ubiquitin-conjugating enzyme E2 variant 1D	m	ID25	0.4	8	0.4	25	1.2	0.5	18	1.3	0.6	21	**1.5**	0.6	16	**1.5**	0.5	9	**1.3**	
UDP-glucose pyrophosphorylase Pyruvate kinase	m, m	ID441; 36	0.4	7	0.4	4	1.1	0.3	18	0.8	0.2	32	**0.6**	0.3	22	0.9	0.4	24	1.0	
Universal stress protein	l	ID9796	0.0	38	0.0	17	0.9	0.0	4	1.0	0.1	104	2.0	0.1	34	**3.6**	0.2	19	**4.8**	
Universal stress protein	l	ID9992	0.0	48	0.0	50	0.7	0.0	10	0.7	0.0	73	2.6	0.1	52	**4.0**	0.2	21	**8.9**	
Urease accessory protein G	s, m	ID750; 18	0.1	13	0.1	6	0.8	0.1	15	1.6	0.2	82	3.6	0.2	59	3.2	0.4	32	**5.8**	
Urease accessory protein G	m	ID17	0.2	31	0.3	23	1.3	0.4	6.6	**2.1**	0.8	58	3.9	0.8	55	4.1	1.2	23	**6.0**	
Voltage-dependent anion channel	m	ID732	2.1	6	2.0	4	1.0	1.9	3	0.9	1.7	9	0.8	1.5	13	0.7	0.9	24	**0.4**	

[a] Proteins were identified via mass spectrometry for spots with the IDs 1–39 (see also Supplementary material 1, Suppl. Table 1 and Suppl. Fig. 1) and using the *Cyclamen persicum* embryo proteome reference map (Rode et al. 2011; http://www.gelmap.de/cyclamen) for all other spots. Proteins which had been identified via mass spectrometry and the proteome reference map resulting in the same protein species are printed in green. Newly identified proteins via MS are printed in red

[b] Molecular weight (MW) in gel as compared to the theoretically expected MW

(m): MW in gel corresponding to the theoretically expected MW ± 15 kDa

(s): MW in gel lower than theoretically expected

(l): MW in gel larger than theoretically expected

[c] Spot ID represents the number of a protein spot in the 2D PAGEs. Corresponding spots of all gels are labelled with the same ID

[d] Mean relative spot volume obtained in the three gels of days 0, 1, 3, 7, 21 or 28. These values are illustrated by graphs at the right side of each line for all shown spots. The first bar (purple) represent day 0 (callus) and the following bars (green) represent the following developmental stages (days 1–28) in chronological order

[e] Coefficient of variation (cov) in percent

[f] Ratio of protein spot abundance (ratio = v (day 1 or day 3 or day 7 or day 21 or day 28)/v (day 0). Statistically significant values of at least 1.5-fold more or 1.5-fold less (all values ≤ 0.6) abundant protein spots are given. Bold printed green figures are indicating values of significant higher abundances in the developing tissue/embryos (days 1–28) as compared to callus. Bold printed purple figures are indicating values of significant lower abundances in the developing tissue/embryos (days 1–28) as compared to callus

Proteins of different abundance in the early developmental stages (1, 3, 7 days: experiment A)

During the early developmental stages (days 1, 3, 7 after transfer to PGR-free medium) in total 39 proteins were found to be differentially abundant compared to callus of which 32 were identified. Within the identified proteins, 15 were of higher abundance in callus. The majority of them was involved in the glycolytic pathway (ID6/ID387), ID36/ID441, ID37, 3ID8) and energy metabolism (ID21, ID24). But also proteins affecting transcription (histone H4; ID19), protein degradation (ubiquitin-40S ribosomal protein S27a-1; ID7) and protein folding (mitochondrial Co-chaperone GrpE family protein; ID31) were of higher abundance in callus. In addition, two catalases (ID389, ID39/ID17829) were more abundant in callus as compared to 7-day-old embryos. Anthocyanidin reductase (ID32), an enzyme representing the flavonoid biosynthesis pathway was found especially in callus and to a lesser extent in all stages of the developing embryos.

In all early developmental stages especially proteins involved in genetic information processing (eukaryotic initiation factor 4A-9: ID15; protein translation factor SUI1, ID26; histone H4: ID8) and protein processing [(prefoldin: ID23/ID1039), HSP 20: ID28 (ID863), HSP 20: ID29/ID897, co-chaperone GrpE: ID3)] were highly abundant. Interestingly, the 26S protease regulatory subunit 6B homolog (ID20) involved in controlled proteolysis was 1.8- to 2.3-fold increased in all early developmental stages. A protein spot containing a HSP 70 protein (ID750) was present in significantly higher amounts in cells 3 days after transfer to PGR-free MS medium and its volume increased with progressing development. Two spots representing small enolase (Rode et al. 2011) (ID981, ID986) were increased in abundance in 7-day-old embryos as compared to callus. Proteins involved in amino acid metabolism (phosphatase 2A, ID14), nitrogen metabolism (urease accessory protein G, ID17, ID18) and stress response (peroxiredoxin, ID4) were more abundant in the early embryo stages than in callus.

Proteins of different abundance in the torpedo-shaped embryos (21, 28 days; experiment A)

The proteomic comparison of callus and torpedo-shaped embryos resulted in an especially high number of alterations. In total, 80 and 173 spots were differentially abundant between callus and 21 and 28-day-old embryos, respectively, the latter representing more than 50% of all spots analysed. These proteins are colour coded in Fig. 2b and spots of special interest are indicated.

Proteins of high abundance in the embryos

The storage protein 7S globulin (ID8764) was specific for the torpedo-shaped embryos. It was first detected in 21-day-old embryos and its volume doubled within 1 week. Additionally, the abundance of the small enolases (ID1020, ID1022, ID1083, ID18597, ID641, ID803, ID8980, ID976, ID981, ID983, ID986, ID997, ID863), which are postulated to be storage compounds (Rode et al. 2011) was high in the older embryos. This group included five spots in the 21-day-old embryos and nine spots in the 28-day-old embryos with a relative spot volume ranging from 1.8- to 24.3-fold as compared to callus. Another interesting protein, an auxin-amidohydrolase (ID853) increased 3.8-fold in the 21-day-old embryos and 10.4-fold in the 28-day-old embryos. The cell division control protein (ID499) was 2.1-fold more abundant in the 21-day-old embryos. The late embryogenesis abundant protein Em (ID1059) as well as the endoribonuclease (ID1057) had an unchanged abundance profile in all developmental stages, except day 28 where they were more than 4 times higher abundant than in previous stages.

Proteins of lower abundance in the embryos

Mitochondrial proteins like succinate dehydrogenase (ID317), voltage-dependent anion channel (ID732) and peptidyl-prolyl *cis–trans* isomerase (ID941) were detected in significantly lower amounts in the embryos as compared to callus. Furthermore, proteins involved in stress response including HSP 20 (ID880), HSP 101 (IDID787) and HSP 60 (ID355), copper/zinc superoxide dismutase (SOD; ID1003) and a stress-inducible protein (ID299) were also of lower abundance in the embryos' proteomes.

Proteins of fluctuating abundance

The catalase spot group appeared in a chain-like arrangement in the upper part of the gels (pI: approximately 7; Fig. 2b) including 4 spots. Of these spots, the two slightly more acidic forms were of higher abundance in embryos of both ages (ID392, ID386). Their volume was low in callus and increased with processing development. The two slightly more basic catalase spots (ID938, ID17829) expressed a reverse accumulation profile. Two protein spots representing a regulatory subunit of the 26S proteasome (ID1970, ID1957) were present in all stages but had an increased abundance in the late embryos (21, 28 days). Interestingly, the volume of one of these spots (ID1970) was equal at the stages 0, 1 and 3 days after transfer to PGR-free MS medium but increased rapidly after 7 days. However, one further ubiquitin spot (ID1194) showed an opposite abundance profile. This spot was highly abundant in the early but less abundant in the late developmental

stages. Ten differentially abundant protein spots were identified as glyceraldehyde-3-phosphate dehydrogenase (GAPDH), four of which were higher and six lower abundant in the embryos. These spots were partly (7 spots) of the expected regular molecular weight and partly their molecular weight was significantly lower in gel than theoretically expected.

Proteins of different abundance in 28-day-old embryos cultivated on MS media with different sucrose levels (experiment A)

The proteomic comparison of 28-day-old embryos cultivated on MS medium containing 60 g l^{-1} sucrose with their counterparts grown on MS medium with 30 g l^{-1} revealed 51 differentially abundant spots, half of which (26) could be identified. These proteins are listed in Table 3 and colour coded in Fig. 3. The embryos exposed to the higher sucrose concentration, exhibited higher levels of 7S globulin and small enolases. Additionally, two very prominent spots in the upper gel part were more than 1.5-fold higher in abundance in these embryos, representing the HSP70. All four catalases were found in approximately 2.5-fold higher abundance in the embryos cultivated with the higher sucrose concentration. Moreover, the cell division control protein had a twofold higher spot volume in theses embryos. HSP 20 and a spot representing voltage-dependent anion channel, a transporter of the outer mitochondrial membrane, were highly present in both embryo types. Peptidase, 26S proteasome and ubiquitin involved in protein processing were lower in abundance in the embryos grown on MS medium containing 60 g l^{-1} sucrose.

Proteins of different abundance in 56-day-old embryos cultivated on MS media with and without ABA (experiment B)

The proteomic comparison of 56-day-old embryos cultivated on MS medium containing 10 mg l^{-1} ABA or no ABA resulted in 43 differentially abundant spots. In total, 15 of these spots could be identified using the proteome reference map published by Rode et al. (2011). These proteins are listed in Table 4 and indicated in Fig. 4. In the proteome of the ABA-treated embryos only two protein types were higher abundant: one spot representing HSP 70 and five spots representing enolase. The enolase spots located in the 15-kDa region of the gels were found to be 1.6- to 6.5-fold increased. Nine proteins were of low abundance in the ABA-treated embryos. These were proteins of the primary metabolism (GAPDH, malatedehydrogenase, ubiquitin), proteins involved in stress response including heat shock proteins (HSP 60, HSP 101) as well as one catalase spot. Glyoxylase, involved in secondary metabolism and polygalacturonase involved in cell wall biogenesis/degeneration were of low abundance in the ABA-treated embryos as well as a spot representing the voltage-dependent anion channel.

Discussion

Which physiological processes are significant during somatic embryogenesis in *Cyclamen persicum*? And is it possible to improve the quality of developed embryos by ABA and high sucrose concentration treatments? To answer these questions the proteomes of six developmental stages were visualised—from callus to torpedo-shaped embryo—during somatic embryogenesis of *C. persicum* via high-resolution 2D-gels. Additionally, the effects of high sucrose concentration and ABA application on the proteomes of somatic embryos were investigated and differentially abundant proteins in response to these maturation-promoting treatments were identified. Distinct proteome structures have been shown to reflect various developmental and physiological processes in plants (Rose et al. 2004).

Easy and fast protein identification via the digital reference map

Using our digital proteome reference map (Rode et al. 2011) a protein identification rate of 40% was achieved (Table 1) for all differentially abundant proteins detected. The number of identified proteins was especially high for the late embryo stages (21 days and later), since the reference map displays the proteome of *C. persicum* zygotic embryos of the same developmental stage. However, for the early developmental stages novel identification by mass spectrometry turned out to be more reasonable.

Callus requires high levels of mitochondrial and glycolytic proteins

Glycolytic enzymes as well as proteins involved in energy metabolism were of increased abundance in callus. In accordance to our study, Lyngved et al. (2008) reported high abundance of carbohydrate and energy supply involved proteins in embryogenic callus of *C. persicum*. Callus, a tissue with a fast growth and high cell division rate, requires high amounts of energy. Thus, an increased supply of metabolites via glycolysis for the TCA cycle and subsequent energy supply via the mitochondrial respiratory chain seems obvious.

Table 3 Proteins of altered abundances in 28-day-old embryos cultivated on MS medium containing different sucrose concentration

Protein name[a]	MW in gel[b]	ID[c]	V (30 g)[d]	V (60 g)[e]	Ratio (30 g/60 g)[f]
30 g L^{-1} sucrose					
HSP20	m	ID880	0.4	0.2	2.2
Fructose-bisphosphate aldolase	m	ID314	0.3	0.2	2.1
Ubiquitin	l	ID9986	0.3	0.2	2.1
Peptidase	m	ID290	0.2	0.1	2.1
Voltage-dependent anion channel	m	ID732	1.5	0.9	1.7
26S proteasome (subunit)	m	ID1970	0.5	0.3	1.7
HSP20	m	ID897	0.7	0.5	1.6
Peptidyl-prolyl *cis–trans* isomerase	m	ID941	1.5	1.0	1.5
60 g L^{-1} sucrose					
Pyruvate kinase	m	ID420	0.2	0.3	0.6
Enolase	m	ID353	0.1	0.2	0.5
Auxin-amidohydrolase	s	ID853	0.8	1.5	0.5
Malate dehydrogenase	m	ID637	0.2	0.4	0.5
Cell division control protein	m	ID139	0.3	0.6	0.5
Catalase	m	ID17829	0.0	0.1	0.4
Catalase	m	ID392	0.2	0.4	0.4
GAPDH	l	ID199	0.4	0.9	0.4
Catalase	m	ID388	0.1	0.1	0.4
HSP20	m	ID911	0.1	0.2	0.4
Catalase	m	ID389	0.1	0.2	0.4
Voltage-dependent anion channel	m	ID858	0.3	1.0	0.3
Enolase	s	ID976	0.0	0.1	0.3
HSP20	l	ID879	0.3	1.0	0.3
7S globulin	s	ID8764	0.2	0.6	0.3
Enolase	s	ID1083	0.1	0.3	0.3
Enolase	s	ID8980	0.0	0.2	0.2

[a] Proteins were identified using the *Cyclamen persicum* embryo proteome reference map (Rode et al. 2011; www.gelmap.de/cyclamen)

[b] Molecular weight (MW) in gel as compared to the theoretically expected MW

(m): MW in gel corresponding to the theoretically expected MW ± 15 kDa

(s): MW in gel lower than theoretically expected

(l): MW in gel larger than theoretically expected

[c] Spot ID represents the unique number of a protein spot in the 2D PAGEs. Corresponding spots of all gels are labelled with the same ID

[d] Mean relative spot volume obtained in the three gels of 28-day-old embryos grown on MS medium containing 30 g l^{-1} sucrose

[e] Mean relative spot volume obtained in the three gels of 28-day-old embryos grown on MS medium containing 60 g l^{-1} sucrose

[f] Ratio of protein spot abundance (ratio = V(30 g)/V(60 g). Statistically significant values of at least 1.5-fold more or 1.5-fold less (all values ≤0.6) abundant protein spots are given

The switch from callus to globular embryo as well as from globular to torpedo-shaped embryo is associated with controlled proteolysis

Subunits of the 26S proteasome and ubiquitin were highly abundant in the globular embryos (days 7–28) but especially noticeable in the late stages (21, 28 days). The ubiquitin/26S proteasome pathway is a major factor in controlled proteolysis: ubiquitinized proteins are recognised and catabolised by the 26S proteasome complex (Sullivan et al. 2003). It has been suggested that the protein breakdown via this pathway plays a key role in plant development by degrading proteins of specific pathways and subsequently supplying amino acids for the biosynthesis of new proteins (Vierstra 1996). In *Arabidopsis*, genes encoding the 26S proteasomal subunit RPN1 were highly expressed in zygotic embryos up to the globular stage. In later developmental stages the expression of these genes rapidly decreased almost down to background level (Brukhin et al. 2005). Additionally, Brukhin et al. (2005)

Table 4 Proteins of altered abundances in 56-day-old embryos cultivated on MS medium with and without ABA

Protein name[a]	MW in gel[b]	ID[c]	V (−ABA)[d]	V (+ABA)[e]	Ratio (+ABA/−ABA)[f]
+ABA					
Enolase	s	ID1032	0.1	0.8	6.5
Enolase	s	ID1083	0.1	0.2	2.4
Enolase	s	ID1022	0.2	0.5	2.3
Enolase	s	ID981	0.4	0.9	2.2
Enolase	s	ID17302	0.2	0.4	1.8
HSP 70	m	ID190	0.2	0.3	1.6
−ABA					
Catalase	m	ID389	0.1	0.1	0.6
Malate dehydrogenase	m	ID1387	0.3	0.1	0.6
GAPDH	m	ID626	0.4	0.2	0.6
Glyoxalase I	m	ID681	0.2	0.1	0.5
Polygalacturonase	m	ID902	0.1	0.0	0.5
HSP 60	m	ID355	0.3	0.1	0.5
Ubiquitin	m	ID810	0.1	0.0	0.3
Voltage-dependent anion channel	m	ID886	0.4	0.1	0.3
HSP 101	m	ID284	0.1	0.0	0.2

[a] Proteins were identified using the *Cyclamen persicum* embryo proteome reference map (Rode et al. 2011; http://www.gelmap.de/cyclamen)

[b] Molecular weight (MW) in gel as compared to the theoretically expected MW

(m): MW in gel corresponding to the theoretically expected MW ± 15 kDa

(s): MW in gel lower than theoretically expected

[c] Spot ID represents the unique number of a protein spot in the 2D PAGEs. Corresponding spots of all gels are labelled with the same ID

[d] Mean relative spot volume obtained in the three gels of 56-day-old embryos grown on MS medium containing 0 mg l^{-1} ABA

[e] Mean relative spot volume obtained in the three gels of 56-day-old embryos grown on MS medium containing 10 mg l^{-1} ABA

[f] Ratio of protein spot abundance (ratio = V(+ABA)/V(−ABA). Statistically significant values of at least 1.5-fold more or 1.5-fold less (all values ≤0.6) abundant protein spots are given

observed that embryos with an RPN1 gene disruption were arrested in the globular stage. The cell division control protein 48 homolog A (CDC48A), which was found in this study in increased abundance in all developmental stages as compared to callus but especially high after 3, 7 and 21 days of differentiation, has been shown to mediate the ubiquitin-26S proteasome pathway (Yen et al. 2000). Aker et al. (2006) reported this enzyme to interact with the somatic embryogenesis receptor like kinase 1 (SERK1). SERK proteins and transcripts have been demonstrated to play a role in somatic embryogenesis in several plant species (e.g., *Arabidopsis*, Hecht et al. 2001; *Medicago*, Nolan et al. 2003) as well as in *Cyclamen* (Rensing et al. 2005; Hönemann et al. 2010). Hönemann et al. (2010) found SERK transcripts to be upregulated in embryogenic callus as compared to non-embryogenic callus of *Cyclamen*. Regarding our results high levels of enzymes involved in the 26S proteasome-dependent proteolysis pathway seem to be important for the switch from callus to globular embryo as well as from globular to torpedo-shaped embryo in *Cyclamen*. A mass spectrometry-based analysis of protein ubiquitination during embryogenesis, as suggested by Saracco et al. (2009), may elucidate the key enzymes involved in the shift of the different developmental stages. On the other hand, a closer look on SERK-mediated protein phosphorylation for the same developmental stages could unravel the enzymes necessary for the subsequent development. The differences in abundance observed for histones (ID8, ID 19) point to the fact that pronounced changes in transcriptional activity are associated with transfer of embryogenic callus to PGR-free medium.

Different HSP levels are stage-specific during embryogenesis

In our study, high levels of HSP20 and HSP70 were representative for differentiated embryos while increased abundances of HSP60 and HSP101 were typical for earlier stages. Heat shock proteins, a family of molecular chaperones, have been reported to be involved in somatic embryogenesis even without being triggered by external

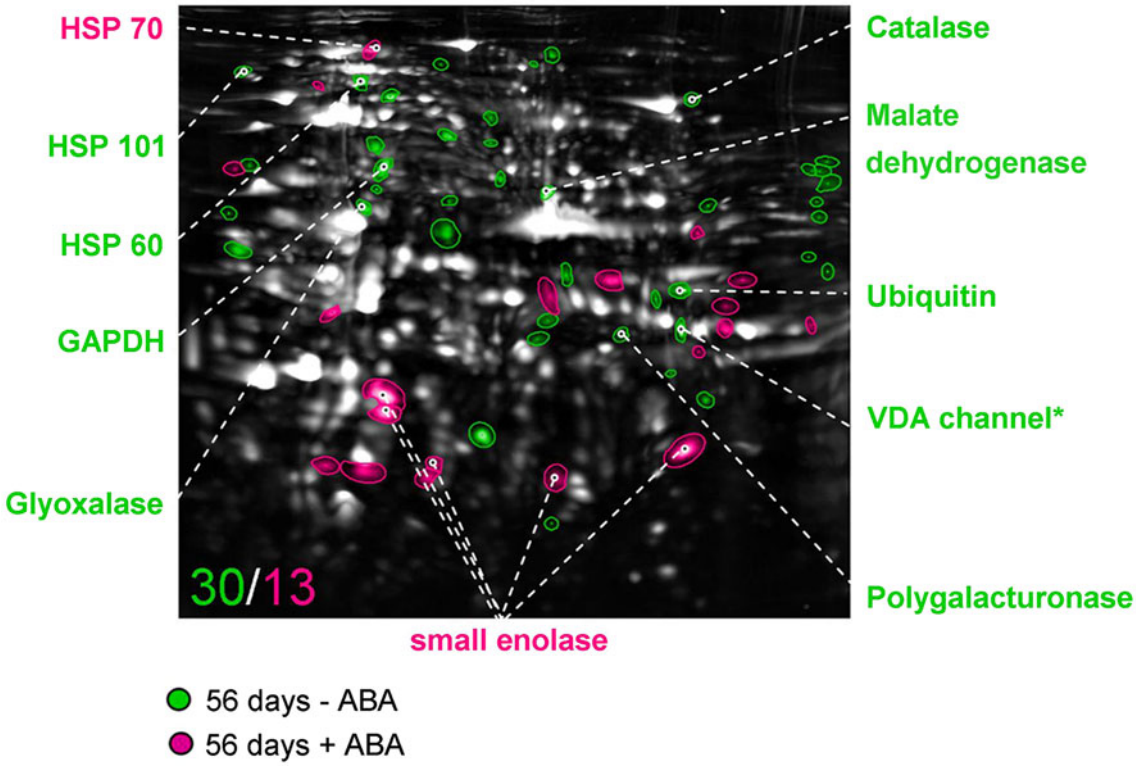

Fig. 4 Alterations in protein abundances in 56-day-old embryos cultivated on MS medium containing different ABA concentrations. Overlay image of IEF SDS-PAGE of 58-day-old embryo proteomes cultivated on MS medium with and without ABA (three replicates, each) using Delta2D software. *Green-labelled* spots were at least 1.5-fold more abundant in the proteome of embryos cultivated without ABA and *pink-labelled* spots were at least 1.5-fold more abundant in the proteome of embryos cultivated with ABA (10 mg l^{-1}). All identified spots are indicated **VDA channel* voltage-dependent anion channel

stresses (Hendrick and Hartl 1993; Waters et al. 1996). In accordance to our study, Pitto et al. (1983) reported a stage-specific accumulation of various HSPs in carrot embryos. Dong and Dunstan (1996) detected transcripts of small HSPs in callus but found them at the highest level in late embryos of white spruce. Puigderrajols et al. (2002) showed small HSPs to be induced in 5-day-old somatic embryos of cork oak. In *Cyclamen*, Winkelmann et al. (2006) found HSP70 to be highly abundant in globular somatic embryos. Rode et al. (2011) identified HSP20, HSP60, HSP70 and HSP101 in zygotic and somatic torpedo-shaped embryos of *C. persicum.* Interestingly, here HSP60 and HSP101 were more abundant in the early somatic embryos while HSP20 and HSP70 were higher abundant in their more mature zygotic counterparts. Similarly, in *Arabidopsis* seeds small HSPs were observed to appear during reserve synthesis at mid-maturation and to decline during germination indicating a possible role in dormancy (Wehmeyer et al. 1996). Taken together, high levels of HSP20 and HSP70 mark late stages of embryogenesis while HSP60 and HSP101 were more typical for earlier stages and callus in *Cyclamen*.

Stage-specific phosphorylation of catalases?

High levels of the more acidic forms of catalases were specific for callus and early stages. In contrast, the more basic forms had a higher abundance in the late embryos. These catalases are therefore candidates for stage-specific isoforms, probably affected by different phosphorylation levels. To our knowledge a similar development-specific pH switch of proteins has not been reported so far for somatic embryogenesis. A MS-based approach to characterise phosphorylated peptides of these proteins could give further insights.

Accumulation of storage compounds occurs in the late stages of embryogenesis

7S globulin was specific for the late embryo stages. It was first detected in 21-day-old embryos and its volume doubled within 1 week. Globulins are a wide spread family of seed storage protein in several plants (for review see Shewry et al. 1995) and have been identified in *Cyclamen* endosperm, zygotic and somatic embryos in earlier studies (Winkelmann et al. 2006; Rode et al. 2011). The putative

novel storage proteins in *Cyclamen*, the small enolases (Rode et al. 2011) were present in all developmental stages but their abundance increased significantly after 28 days of differentiation. Thus, the first storage proteins are partly present in high levels after 3 weeks and their amount significantly increased after 28 days of differentiation in *Cyclamen* embryos. The synthesis of large amounts of storage compounds is a marker for embryo maturation.

Release of endogenous auxin in the late stages of embryogenesis?

High levels of auxin-amidohydrolase were typical for the older developmental stages and this enzyme also exhibited an increased abundance in embryos grown on high sucrose MS medium. Auxin-amidohydrolases release active auxin (indole-3-acetic acid) by hydrolysing auxin-storage conjugates in plant cells (for review see Bajguz and Piotrowska 2009). High levels of auxin-amidohydrolase have been shown to be characteristic for torpedo-shaped zygotic embryos of *C. persicum* and less abundant in their somatic counterparts (Rode et al. 2011). Auxins are a group of plant growth regulators with various functions. They promote cell elongation, division and differentiation (Teale et al. 2006). It has been shown that endogenous indole-3-acetic acid is essential in embryogenic patterning (Weijers et al. 2006) as well as in post embryogenic development (Geldner et al. 2004) and germination (Rampey et al. 2004). Weijers and Jürgens (2005) reported the accumulation of auxin at specific positions that correlate with developmental decisions in early embryogenesis (up to globular stage). Michalczuk et al. (1992) found significantly lower levels of indole-3-acetic acid in late embryo stages of carrot. Thus, high auxin levels are not characteristic for late embryos and the putative increase of endogenous auxin evoked by auxin-amidohydrolase in this development stages needs further investigation in *Cyclamen*. Here, the role of auxins is assumed most likely by stimulating cell elongation in the growing embryo. The abundance of this enzyme should be correlated to measured auxin contents for the analysed different developmental stages of somatic embryogenesis in *Cyclamen*. The auxin-amidohydrolase may, however, be considered as a candidate marker protein for mature embryos.

High sucrose levels and ABA treatment promote the maturation of somatic embryos

Proteins correlated with maturation processes like storage compounds (7S globulin, small enolases), HSP70 (see above) and auxin-amidohydrolase (see above) occurred more abundantly in the proteomes of 28-day-old embryos exposed to the higher sucrose level. The main effect of ABA on the proteome of 56-day-old embryos was the pronounced increase of the putative storage compounds small enolases. One further interesting protein, occurring in high abundance starting from day 28 in both sucrose variants was the Em-like protein. The Em protein is an osmoprotective molecule of the late embryogenesis abundant (LEA) class (Swire-Clark and Marcotte 1999). All these proteins have been shown to be highly abundant in torpedo-shaped zygotic embryos of *Cyclamen* (Rode et al. 2011). We assume that a proteome structure close to the one of zygotic embryos is supposed to reflect high-quality somatic embryos in *Cyclamen* (Rode et al. 2011). Additionally, enzymes involved in the primary metabolism were decreased in ABA-treated embryos. This is a hint for inchoate maturation and probably also dormancy. In accordance to our study, maturation-promoting effects of ABA (Gutmann et al. 1996; Garcia-Martin et al. 2005; Vahdati et al. 2008; Sghaier-Hammami et al. 2010) and high sucrose levels (Klimaszewska et al. 2004; Winkelmann et al. 2006; Sghaier-Hammami et al. 2010) have been reported for various plants. However, the raised abundance of catalases in embryos grown on the high sucrose medium may indicate increased oxidative stress, triggered by osmotic pressure. Though, the cultivation on MS medium including 60 g l^{-1} sucrose as well as the ABA treatment seems to have desirable effects on the proteome structure by becoming more analogous to the zygotic "ideal" status. Probably, the combination of both factors, embryogenesis on MS medium containing 60 g l^{-1} sucrose and a subsequent maturation step by ABA treatment may result in even more mature embryos. However, on the morphological level we could not detect any significant differences between ABA-treated embryos and their counterparts grown on PGR-free MS medium. ABA application in earlier developmental stages like performed by Vahdati et al. (2008) for 1-week-old walnut somatic embryos or a stepwise ABA treatment to mimic the natural level in seeds may improve the positive effects of this PGR on embryo maturation and quality.

Conclusions and outlook

In our study major physiological processes of embryogenesis in *Cyclamen* were elucidated. Thus, the first question stated at the beginning of our discussion could be answered. However, now a number of new questions arise: (1) which proteins are ubiquitinated and phosphorylated during developmental decision from callus to globular embryo and from globular to torpedo-shaped embryo? (2) Are there stage-specific isoforms of catalase? (3) Is there a *Cyclamen*-specific auxin accumulation profile? To resolve the new questions concerning post-translational modifications a gel- or mass spectrometry-based approach like performed by

Trapphoff et al. (2009) or Grimsrud et al. (2010) could be helpful. A metabolic profiling of auxin levels in the different stages of embryogenesis of *Cyclamen* could elucidate the dynamics of this plant hormone and its correlation to auxin-amidohydrolase and auxin-storage conjugates. The positive effects of high sucrose and ABA treatment for embryo maturation have been demonstrated. Thus, also the second question could be answered. However, the optimal time-point as well as concentration of ABA application should be investigated in greater detail in further studies.

Acknowledgments The authors would like to thank Dr. Frank Colditz, Institute of Plant Genetics, Leibniz Universitaet Hannover, for proof reading and critical discussion, Jenniffer Mwangi for proof reading, Michael Senkler for computer-related assistance and the DFG (German research foundation) for financial support.

References

Aker J, Borst JW, Karlova R, de Vries S (2006) The *Arabidopsis thaliana* AAA protein CDC48A interacts in vivo with the somatic embryogenesis receptor-like kinase 1 receptor at the plasma membrane. J Struc Biol 156:62–71

Bajguz A, Piotrowska A (2009) Conjugates of auxin and cytokinin. Phytochemistry 70:957–969

Brukhin V, Gheyselincka J, Gagliardinia V, Genschikb P, Grossniklaus U (2005) The RPN1 subunit of the 26S proteasome in *Arabidopsis* is essential for embryogenesis. Plant Cell 17:2723–2737

Colditz F, Braun HP, Jacquet C, Niehaus K, Krajinski F (2005) Proteomic profiling unravels insights into the molecular background underlying increased *Aphanomyces euteiches* tolerance of *Medicago truncatula*. Plant Mol Biol 59:387–406

Dong JZ, Dunstan DI (1996) Expression of abundant mRNAs during somatic embryogenesis of white spruce [*Picea glauca* (Moench) Voss]. Planta 199:459–466

Garcia-Martin G, Manzanera JA, Gonzalez-Benito ME (2005) Effect of exogenous ABA on embryo maturation and quantification of endogenous levels of ABA and IAA in *Quercus suber* somatic embryos. Plant Cell Tissue Org Cult 80:171–177

Geldner N, Richter S, Vieten A, Marquardt S, Torres-Ruiz RA, Mayer U, Jürgens G (2004) Partial loss-of-function alleles reveal a role for *GNOM* in auxin transport-related, postembryonic development of *Arabidopsis*. Development 131:389–400

Grimsrud PA, den Os D, Wenger CD, Swaney DL, Schwartz D, Sussman MR, Ané JM, Coon JJ (2010) Large-scale phosphoprotein analysis in *Medicago truncatula* roots provides insight into in vivo kinase activity in legumes. Plant Physiol 152:19–28

Gutmann M, von Aderkas P, Label P, Lelu AM (1996) Effects of abscisic acid on somatic embryo maturation of hybrid larch. J Exp Bot 305:1905–1917

Hajduch M, Ganapathy A, Stein JW, Thelen JJ (2005) A systematic proteomic study of seed filling in soybean: establishment of high resolution two-dimensional reference maps, expression profiles, and an interactive proteome database. Plant Physiol 137:1397–1419

Hecht V, Vielle-Calzada JP, Hartog MV, Schmidt EDL, Boutilier K, Grossniklaus U, de Vries SC (2001) The Arabidopsis *Somatic Embryogenesis Receptor Kinase 1 Gene* is expressed in developing ovules and embryos and enhances embryogenic competence in culture. Plant Physiol 127:803–816

Hendrick JP, Hartl FU (1993) Molecular chaperone functions of heat-shock proteins. Annu Rev Biochem 62:349–384

Hönemann C, Richardt S, Krüger K, Zimmer AD, Hohe A, Rensing SA (2010) Large impact of the apoplast on somatic embryogenesis in *Cyclamen persicum* offers possibilities for improved developmental control in vitro. BMC Plant Biol 10:77

Hurkman WJ, Tanaka CK (1986) Solubilization of plant membrane proteins for analysis by two dimensional gel electrophoresis. Plant Physiol 8:802–806

Imin N, Nizamidin M, Daniher D, Nolan KE, Rose RJ, Rolfe BG (2005) Proteomic analysis of somatic embryogenesis in *Medicago truncatula*. Explant cultures grown under 6-benzylaminopurine and 1-naphthaleneacetic acid treatments. Plant Physiol 137:1250–1260

Kiviharju E, Tuominen U, Törmälä T (1992) The effect of explant material on somatic embryogenesis of *Cyclamen persicum* Mill. Plant Cell Tissue Organ Cult 28:187–194

Klimaszewska K, Morency F, Jones-Overton C, Cooke J (2004) Accumulation pattern and identification of seed storage proteins in zygotic embryos of *Pinus strobus* and in somatic embryos from different maturation treatments. Physiol Plant 121:682–690

Lippert D, Zhuang J, Ralph S, Ellis DE, Gilbert M, Olafson R, Ritland K, Ellis B, Douglas CJ, Bohlmann J (2005) Proteome analysis of early somatic embryogenesis in *Picea glauca*. Proteomics 5:461–473

Lyngved R, Renaut J, Hausman JF, Iversen TH, Hvoslef-Eide AK (2008) Embryo specific proteins in *Cyclamen persicum* analyzed with 2-D DIGE. J Plant Growth Regul 27:353–369

Marsoni M, Bracale M, Espen L, Prinsi B, Negri AS, Vannini C (2008) Proteomic analysis of somatic embryogenesis in *Vitis vinifera*. Plant Cell Rep 27:347–356

Mauri PV, Manzanera JA (2003) Induction, maturation and germination of holm oak (*Quercus ilex* L.) somatic embryos. Plant Cell Tissue Organ Cult 74:229–235

Michalczuk L, Cooke J, Cohen JD (1992) Auxin levels at different stages of carrot somatic embryogenesis. Int J Plant Biochem 31:1097–1103

Mihr C, Braun HP (2003) Proteomics in plant biology. In: Michael P (ed) Handbook of proteomics methods. Humana, Totowa, pp 409–416

Murashige T, Skoog F (1962) A revised medium for rapid growth and bioassays with tobacco tissue cultures. Physiol Plant 15:473–497

Neuhoff V, Stamm R, Eibl H (1985) Clear background and highly sensitive protein staining with Coomassie Blue dyes in polyacrylamide gels: a systematic analysis. Electrophoresis 6:427–448

Neuhoff V, Stamm R, Pardowitz I, Arold N, Ehrhardt W, Taube D (1990) Essential problems in quantification of proteins following colloidal staining with Coomassie Brilliant Blue dyes in polyacrylamide gels, and their solution. Electrophoresis 11:101–117

Nolan KE, Irwanto RR, Rose RJ (2003) Auxin up-regulates *MtSERK1* expression in both *Medicago truncatula* root-forming and embryogenic cultures. Plant Physiol 133:218–230

Pitto L, Lo Schiavo F, Giuliano G, Terzi M (1983) Analysis of the heat-shock protein pattern during somatic embryogenesis of carrot. Plant Mol Biol 2:231–237

Prange ANS, Serek M, Bartsch M, Winkelmann T (2010a) Efficient and stable regeneration from protoplasts of *Cyclamen coum* Miller via somatic embryogenesis. Plant Cell Tiss Org Cult 101:171–182

Prange ANS, Bartsch M, Serek M, Winkelmann T (2010b) Regeneration of different *Cyclamen* species via somatic embryogenesis from callus, suspension cultures and protoplasts. Sci Hortic 125:442–450

Puigderrajols P, Jofre A, Mir G, Pla M, Verdaguer D, Huguet G, Molinas M (2002) Developmentally and stress-induced small

heat shock proteins in cork oak somatic embryos. J Exp Bot 53:1445–1452

Rampey RA, LeClere S, Kowalczyk M, Ljung K, Sandberg G, Bartel B (2004) A family of auxin-conjugate hydrolases that contributes to free indole-3-acetic acid levels during *Arabidopsis* germination. Plant Physiol 135:978–988

Rensing SA, Lang D, Schumann E, Reski R, Hohe A (2005) EST sequencing from embryogenic *Cyclamen persicum* cell cultures identifies a high proportion of transcripts homologous to plant genes involved in somatic embryogenesis. J Plant Growth Regul 24:102–115

Rode C, Gallien S, Heintz D, Van Dorsselaer A, Braun HP, Winkelmann T (2011) Enolases: storage compounds in seeds? Evidence from a proteomic comparison of zygotic and somatic embryos of *Cyclamen persicum* Mill. Plant Mol Biol 75:305–319

Rose JKC, Bashir S, Giovannoni JJ, Jahn MM, Saravanan RS (2004) Tackling the plant proteome: practical approaches, hurdles and experimental tools. Plant J 39:715–773

Saracco SA, Hansson M, Scalf M, Walker JM, Smith LM, Vierstra RD (2009) Tandem affinity purification and mass spectrometric analysis of ubiquitylated proteins in *Arabidopsis*. Plant J 59:344–358

Schmidt T, Ewald A, Seyring M, Hohe A (2006) Comparative analysis of cell cycle events in zygotic and somatic embryos of *Cyclamen persicum* indicates strong resemblance of somatic embryos to recalcitrant seeds. Plant Cell Rep 25:643–650

Schwenkel HG, Winkelmann T (1998) Plant regeneration via somatic embryogenesis from ovules of *Cyclamen persicum* Mill. Plant Tiss Cult Biotechnol 4:28–34

Sghaier-Hammami B, Jorrín-Novo JV, Gargouri-Bouzid R, Drira N (2010) Abscisic acid and sucrose increase the protein content in date palm somatic embryos, causing changes in 2-DE profile. Phytochemistry 71:1223–1236

Shewry PR, Napier JA, Tatham AS (1995) Seed storage proteins: structures and biosynthesis. Plant Cell 7:945–956

Sullivan JA, Shirasu K, Deng XW (2003) The diverse roles of ubiquitin and the 26S proteasome in the life of plants. Nat Rev Genet 4:948–958

Swire-Clark GA, Marcotte WR (1999) The wheat LEA protein Em functions as an osmoprotective molecule *in Saccharomyces cerevisiae*. Plant Mol Biol 39:117–128

Teale WD, Paponov IA, Palme K (2006) Auxin in action: signalling, transport and the control of plant growth and development. Nature Rev Mol Cell Biol 7:847–859

Trapphoff T, Beutner C, Niehaus K, Colditz F (2009) Induction of distinct defense-associated protein patterns in *Aphanomyces euteiches* (Oomycota)-elicited and -inoculated *Medicago truncatula* cell-suspension cultures: a proteome and phosphoproteome approach. Mol Plant-Microbe Interact 22:421–436

Vahdati K, Bayat S, Ebrahimzadeh H, Jariteh M, Mirmasoumi M (2008) Effect of exogenous ABA on somatic embryo maturation and germination in Persian walnut (*Juglans regia* L.). Plant Cell Tissue Organ Cult 93:163–171

Vierstra RD (1996) Proteolysis in plants: mechanisms and functions. Plant Mol Biol 32:275–302

Waters ER, Lee GJ, Vierling E (1996) Evolution, structure and function of the small heat shock proteins in plants. J Exp Bot 47:325–338

Wehmeyer N, Hernandez LD, Finkelstein RR, Vierling E (1996) Synthesis of small heat-shock proteins is part of the developmental program of late seed maturation. Plant Physiol 112: 747–757

Weijers D, Jürgens G (2005) Auxin and embryo axis formation: the ends in sight? Curr Opin Plant Biol 8:32–37

Weijers D, Schlereth A, Ehrismann JS, Schwank G, Kientz M, Jürgens G (2006) Auxin triggers transient local signaling for cell specification in *Arabidopsis* embryogenesis. Dev Cell 10:265–270

Wicart G, Mouras A, Lutz A (1984) Histological study of organogenesis and embryogenesis in *Cyclamen persicum* tissue cultures: evidence for a single organogenetic pattern. Protoplasma 119:159–167

Winkelmann T, Hohe A, Schwenkel HG (1998) Establishing embryogenic suspension cultures in *Cyclamen persicum* 'Purple Flamed'. Adv Hortic Sci 12:25–30

Winkelmann T, Meyer L, Serek M (2004) Desiccation of somatic embryos of *Cyclamen persicum* Mill. J Hortic Sci Biotechnol 79:479–483

Winkelmann T, Heintz D, Van Dorsselaer A, Serek M, Braun HP (2006) Proteomic analyses of somatic and zygotic embryos of *Cyclamen persicum* Mill. reveal new insights into seed and germination physiology. Planta 224:508–519

Yen CH, Yang YC, Ruscetti SK, Kirken RA, Dai RM, Li CCH (2000) Involvement of the ubiquitin–proteasome pathway in the degradation of nontyrosine kinase-type cytokine receptors of IL-9, IL- 2, and erythropoietin. J Immunol 165:6372–6380